catalysts

MDPI

Article

Regarding the Nature of Charge Carriers Formed by UV or Visible Light Excitation of Carbon-Modified Titanium Dioxide

Arsou Arimi [1,*,†], Carsten Günnemann [1,*,†], Mariano Curti [1,*] and Detlef W. Bahnemann [1,2,3]

1 Institut für Technische Chemie, Gottfried Wilhelm Leibniz Universität Hannover, Callinstrasse 3, 30167 Hannover, Germany
2 Laboratorium für Nano- und Quantenengineering, Gottfried Wilhelm Leibniz Universität Hannover, Schneiderberg 39, 30167 Hannover, Germany
3 Laboratory "Photoactive Nanocomposite Materials", Saint-Petersburg State University, Ulyanovskaya str. 1, Peterhof, 198504 Saint Petersburg, Russia
* Correspondence: arimi@iftc.uni-hannover.de (A.A.); guennemann@iftc.uni-hannover.de (C.G.); curti@iftc.uni-hannover.de (M.C.); Tel.: +49(0)511-762-2773 (A.A., C.G. & M.C.)
† These two authors contributed equally to this work.

Received: 1 August 2019; Accepted: 17 August 2019; Published: 20 August 2019

Abstract: Although titanium dioxide gathers many of the required properties for its application in photocatalytic processes, its lack of activity in the visible range is a major hurdle yet to be overcome. Among different strategies, the post-synthesis modification of TiO_2 powders with organic compounds has already led to commercially available materials, such as KRONOClean 7000. In this work, we apply diffuse reflectance transient absorption spectroscopy on this visible-light active photocatalyst and study the dynamics of the charge carriers alternatively induced by UV or visible light laser irradiation, under inert or reactive atmospheres. Our results can be interpreted by considering the material as TiO_2 sensitized by an organic-based layer, in agreement with previous studies on it, and show that the oxidative power of the material is considerably diminished under visible light irradiation. By complementarily performing continuous visible light irradiation photocatalysis experiments in aerated aqueous suspensions, we show that, although the oxidation of methanol proceeds at a very slow rate, the oxidation of chlorpromazine occurs much faster thanks to its better suited redox potential.

Keywords: visible light driven photocatalysis; KRONOClean 7000; carbon-based modified TiO_2; transient absorption spectroscopy; chlorpromazine; carbon-doped materials

1. Introduction

In 1972, Fujishima and Honda reported the photocatalytic splitting of water over titanium dioxide (TiO_2) photoelectrodes irradiated with UV light [1]. Since this discovery, much work has been done to understand the underlying processes in photocatalytic reactions [2] and develop new materials with activity in the visible range [3]. Despite these efforts, TiO_2 continues to be the most employed photocatalyst, in particular in its anatase polymorph, due to its higher activity in comparison with the thermodynamically stable form rutile [4,5]. However, anatase has a bandgap of 3.23 eV [6] and, thus, it can make use of not more than 3.5% of the energy emitted by the sun [7]. Different strategies have been considered to increase this fraction. One possibility is to replace the material altogether. For example, iron based photocatalysts generally show a strong absorption in the visible range; however, they are far less active under visible light irradiation than TiO_2 under UV irradiation [8,9]. Besides its replacement

with other photocatalysts, a range of different approaches can be used to enhance the light absorption by TiO_2, such as doping or the adsorption of sensitizers on the surface. While doping of TiO_2 (either with metals or non-metals) typically leads to bandgap narrowing [10,11], dye-sensitization extends the visible-light response by coupling the semiconductor with a strongly absorbing molecule, finding applications not only in the field of solar cells [12], but also for photocatalysis [13,14]. These attempts can be considered successful after the commercial development of the KRONOClean 7000 photocatalyst from Kronos International, synthesized by the modification of TiO_2 with pentaerythritol [15]. Although initially it was thought to be carbon-doped TiO_2, it was later proven to consist of anatase particles with a carbon-based sensitizer layer around them [15]. By performing a set of simple but elegant experiments, Ząbek et al. were able to remove the layer around the particles and to reassemble it afterwards, while getting exactly the same properties as before the removal. Importantly, the material was shown to be superior to Evonik P25, both for the photocatalytic abatement of NO_x under white light excitation and for the degradation of acetone under visible light [16,17]. Nevertheless, to the best of our knowledge, the tradeoffs incurred by extending the photocatalytic activity of TiO_2 to the visible range, and the similarities or differences of this process compared to those initiated with UV light, remain so far unclarified.

With the goal of understanding the nature and reactivity of its photogenerated charge carriers, here we investigated KRONOClean 7000 by means of transient absorption spectroscopy using both UV (355 nm) and visible light (455 nm) laser excitation. Furthermore, we analyzed the influences of inert (argon), oxygen, and methanol atmospheres on the charge carrier dynamics. Complementarily, we studied the photocatalytic oxidation of two organic compounds, chlorpromazine and methanol, using aerated KRONOClean 7000 suspensions under continuous visible light irradiation, from which we were able to establish boundaries on its photocatalytic activity under such conditions.

2. Results

2.1. Characterization of the Photocatalyst

We start the material characterization by analyzing the basic structural properties of KRONOClean 7000 (from here on, K-7000). As can be observed in Figure 1, the XRD pattern matches well with the standard data of anatase TiO_2 (JCPDS card No. 21-1272), indicating that the carbon modification does not significantly modify the crystalline structure of the parent material. The pattern precludes the presence of a significant fraction of the rutile or brookite TiO_2 polymorphs.

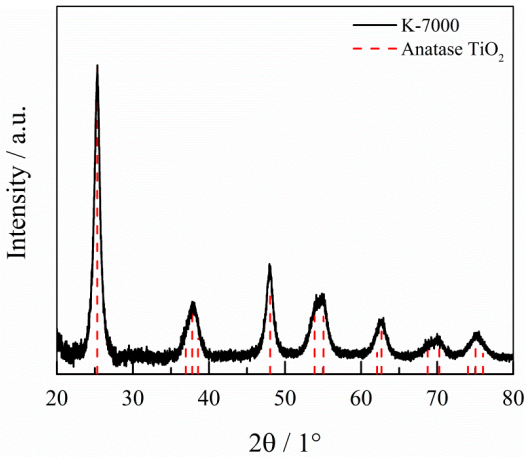

Figure 1. XRD pattern of K-7000 and the anatase reference JCPDS card No. 21-1272.

To determine the light absorbing properties of the photocatalyst, we measured its diffuse reflectance spectra in the spectral range from 300 to 800 nm (Figure 2a). As a comparison, the results for the pure-anatase photocatalyst Hombikat UV100 are also shown. From these spectra, we determined

the Kubelka–Munk functions, shown in Figure 2b. A long-tailed absorption is clearly observed for K-7000, spanning the visible range from 400 nm to 550 nm. On the contrary, UV100 only absorbs in the ultraviolet range. By processing the spectra of K-7000 and Hombikat UV100 with the Tauc plot (Figure S1) we obtained bandgap values of 3.31 eV (corresponding to a wavelength of 374 nm) for K-7000 and 3.32 eV (~373 nm) for UV100.

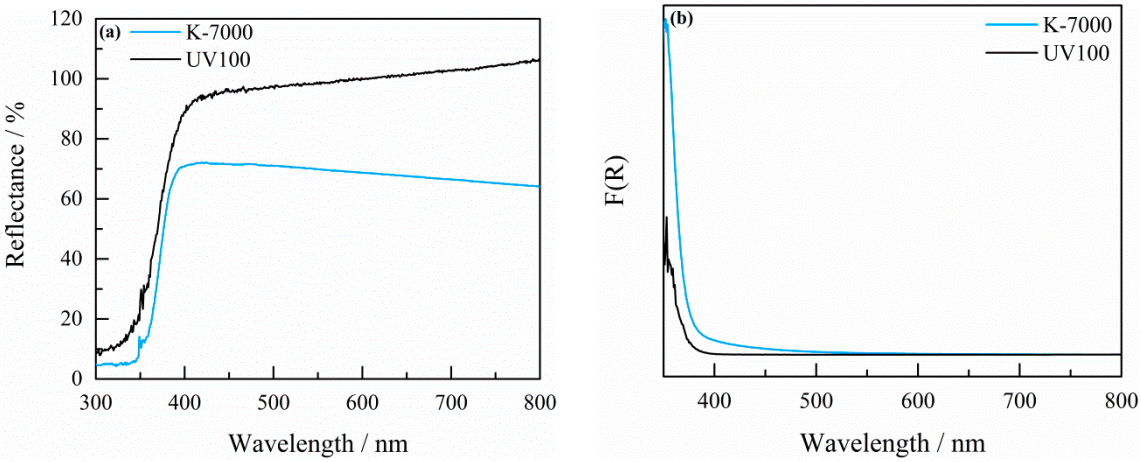

Figure 2. (**a**) Diffuse reflectance spectra (DRS) and (**b**) Kubelka–Munk functions of K-7000 and Hombikat UV100.

2.2. Mott–Schottky Measurements

In order to determine the flatband potential of K-7000 and Hombikat UV100, we performed electrochemical measurements. By plotting the inverse of the square of the measured capacitance versus the applied potential, the flatband potential can be obtained by a linear fit. As shown in Figure 3, this value was determined to be equal to −0.46 V vs. NHE and −0.51 V vs. NHE, for K-7000 and Hombikat UV100, respectively. The small difference is within experimental error.

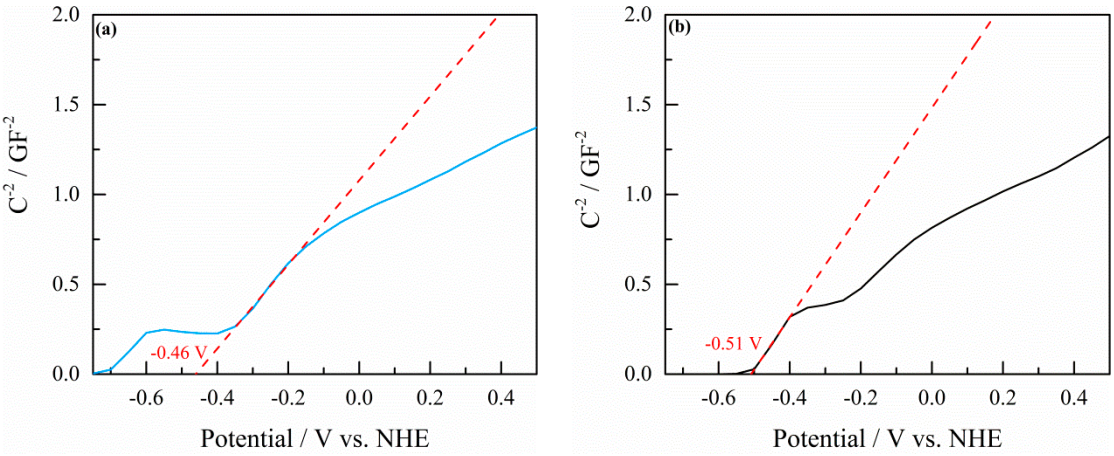

Figure 3. Mott–Schottky plot of (**a**) a K-7000 film and (**b**) a Hombikat UV100 film measured in a 0.1 M KNO_3 solution at a frequency of 100 Hz. The dashed red line shows the extrapolation of the linear part to the ordinate value of zero.

2.3. Transient Absorption Spectroscopy

To study the dynamics of the photogenerated charge carriers, we investigated K-7000 via diffuse reflectance transient absorption spectroscopy. Figure 4 presents the transient absorption spectra of the K-7000 powder obtained after excitation with 355 nm (Figure 4a) and 455 nm (Figure 4b) at 100 ns after the laser excitation. The spectra were obtained at three different conditions, as follows: in the presence

of oxygen (electron scavenger), of methanol (hole scavenger), and in the absence of electron scavengers or donors (Ar atmosphere). In the latter case, the photogenerated charge carriers can only react with each other (i.e., recombine).

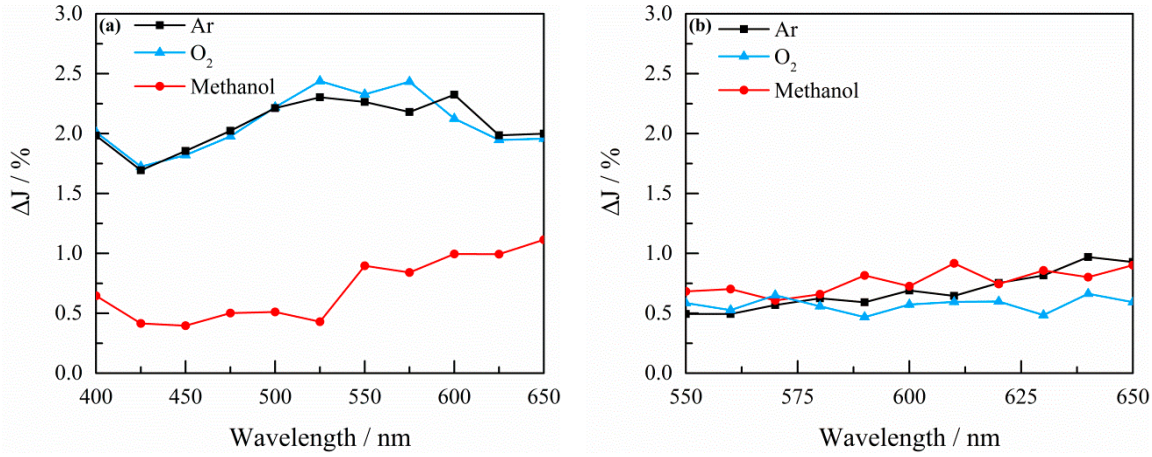

Figure 4. Transient absorption spectra of K-7000 measured 100 ns after excitation with a (**a**) 355 nm and (**b**) 455 nm laser in Ar (black), O_2 (blue), and methanol (red) atmospheres.

As can be seen in Figure 4a, after excitation with 355 nm, there are no significant differences in the transient absorption spectra under Ar or O_2 atmospheres, while the experiments in Ar atmosphere and methanol atmosphere show a considerable difference. Moreover, this difference is larger at shorter wavelengths (~400 nm) than at the longer wavelength range (~650 nm). On the other hand, as revealed in Figure 4b, the transient absorption spectra obtained after excitation with 455 nm in all the atmospheres are, within experimental error, identical to each other.

Figure 5 displays the transient absorption decays detected at 650 nm for the K-7000 powder in O_2, methanol and Ar atmospheres after excitation with 355 nm (left) and 455 nm (right). In the case of excitation with 355 nm (Figure 5a), both under Ar and O_2 atmospheres the transient absorption strongly increases right after the laser pulse and is followed by a rapid decrease down to ~15% of the initial value at 8 µs. In the case of the methanol atmosphere, however, the transient absorption is initially lower than the other two cases and increases with time in the investigated window. By comparing the transient absorption decays after excitation with 355 nm and 455 nm, Figure 5a,b, it can be seen that the initial absorptions after excitation with 455 nm are much lower than those values after excitation with 355 nm. After excitation with 455 nm the decrease of the transient absorption is significantly slower and decreases only to ~60% of the initial value after 8 µs. Furthermore, at this excitation wavelength no significant difference was observed regarding the type of atmosphere.

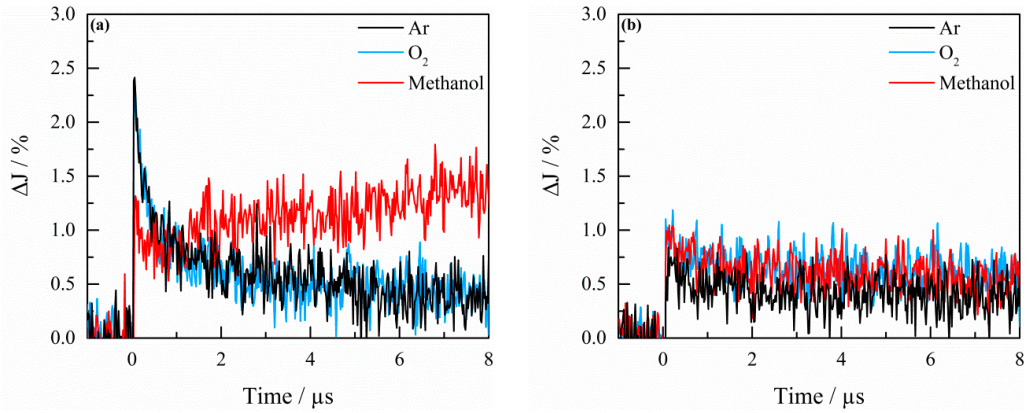

Figure 5. Transient absorption decays of K-7000 detected at 650 nm in an Ar (black), an O_2 (blue), and a methanol (red) atmosphere, after excitation with (**a**) 355 nm and (**b**) 455 nm.

The behavior of K-7000 under visible-light excitation was compared with that of Hombikat UV100 in Ar atmosphere. Figure 6a shows the transient absorption decays in K-7000 and UV100 powders detected at 650 nm, after excitation with 455 nm. While UV100 shows virtually no transient absorption, a significant signal with a long-lived component can be observed for K-7000. Similarly, the transient absorption spectrum of UV100 (Figure 6b) at 100 ns after the pulse is negligible with respect to that of K-7000.

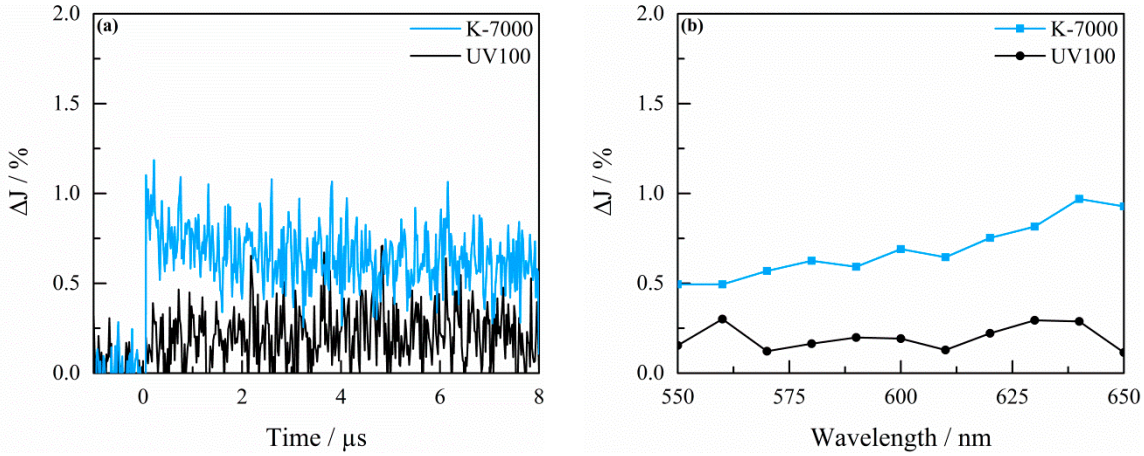

Figure 6. (**a**) Transient absorption decays of K-7000 (blue) and UV100 (black) observed at 650 nm in an Ar atmosphere after excitation with 455 nm, (**b**) transient absorption spectra of K-7000 (blue) and UV100 (black) measured at 100 ns after the laser excitation.

2.4. Photocatalytic Experiments

In order to evaluate the visible-light activity of K-7000, we performed photocatalytic experiments using methanol and chlorpromazine as organic model compounds. For that matter, we analyzed their conversion in the presence of a K-7000 suspension upon irradiation at 455 nm. The results of these experiments are shown in Figure 7.

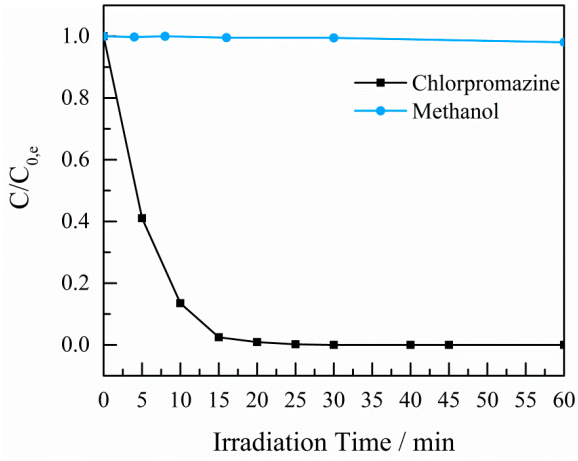

Figure 7. Comparison of the conversion of methanol and chlorpromazine upon visible light irradiation (455 nm) in the presence of K-7000.

The oxidation of methanol was monitored by assessing the production of formaldehyde throughout the reaction period (Figure S2). After 60 min of visible light irradiation in the presence of K-7000, only a slight degradation of methanol was observed.

In the case of chlorpromazine, it was found to be stable in the absence of K-7000 throughout the photolytic reaction time (Figure S3) under visible light irradiation (455 nm), as expected from

the very low overlap between its absorption spectrum and the emission spectrum of the light source (Figure S4). In the presence of K-7000, however, chlorpromazine is completely converted within the first 30 min of irradiation. The main product of this reaction is chlorpromazine sulfoxide, identified by comparing its retention time with a standard sample. The sulfoxide seems to be stable with respect to its photocatalytic conversion, since its concentration increases monotonically before reaching a constant value at ~30 min (Figure S5). As a comparison, we have also investigated the photocatalytic conversion of chlorpromazine in the presence of Hombikat UV100 under visible light irradiation under identical conditions. However, in this case, the conversion of chlorpromazine was negligible (Figure S6).

3. Discussion

The XRD analysis of the K-7000 powder (Figure 1) confirms that anatase is the only crystalline phase significantly present, as also reported by Ząbek et al. [15]. Thus, no effect of the carbon-based layer on the crystalline structure of the titanium dioxide is observed. The anatase phase of the photocatalyst was further evinced by the UV-vis reflectance measurements (Figure 2a). From these, a bandgap value of 3.31 eV was found (Figure S1), which was in good agreement with previous reports [15,17]. Moreover, the comparison of the absorption properties of K-7000 with those of UV100 (pure anatase) reveals a broad absorption band in the visible region for K-7000, not observed in anatase and, thus, ascribed to the carbon-based layer. The flatband potential of K-7000 was determined via Mott–Schottky measurements to be −0.46 V vs. NHE at pH 7 (Figure 3a), similar to a previously reported value for its quasi-Fermi level (−0.50 V vs. NHE at pH 7) [15]. Both values match very well with those measured for anatase TiO_2 (Hombikat UV100) and, therefore, it can be concluded that the modification performed on K-7000 does not significantly affect the position of its conduction band.

Transient absorption spectroscopy measurements were performed in different atmospheres using excitation with UV light (355 nm) and visible light (455 nm). In the Ar atmosphere the only possible fate of the photogenerated charge carriers is recombination with each other, since no other species are present to react with them. Since oxygen can act as an electron scavenger, it would be expected for it to affect the transient absorption spectra and decays. However, no difference can be observed between inert and O_2 atmospheres in both transient absorption spectra and transient decays, irrespective of the excitation wavelength. The standard reduction potential of oxygen is −0.33 V vs. NHE [18], i.e., more positive than the flatband potential of K-7000 (−0.46 V vs. NHE in neutral solution). Therefore, from a thermodynamic point of view, the transfer of electrons from the conduction band of TiO_2 to oxygen molecules is expected to happen. The scavenging of photogenerated electrons in TiO_2 by O_2 molecules in the gas atmosphere has been studied by Yamakata et al., who found a characteristic reaction time of tens of microseconds. Consequently, no significant reaction can be observed before 10 µs [19]. Accordingly, O_2 shall not affect the transient absorption spectra in the considered time scale. For longer time scales it would be possible to observe an effect of the O_2 atmosphere; however, our focus is on the oxidative half-reaction, and thus, for consistency, we limited ourselves to an 8 µs window.

Methanol is a well-known hole scavenger and reacts in a first step to form an α-hydroxyl radical (Equation (1)) [20,21]. For this oxidation reaction, a potential of 1.03 V vs. NHE is required at pH 7 [22]. With the flatband potential of −0.46 V vs. NHE and the determined bandgap of 3.31 eV, the valence band edge can be calculated to be at 2.85 V vs. NHE. For the abstraction of an electron from a methanol molecule, the valence band edge and thus the potential of the photogenerated holes must be more positive compared to the redox potential of the methanol oxidation. Accordingly, this reaction is likely to take place. In general, a transient absorption spectrum contains contributions from both, photogenerated electrons and holes. Herein, methanol acts as a hole scavenger; therefore, only the spectrum of the remaining electrons can be detected. Furthermore, since there is no electron scavenger present, photogenerated electrons accumulate in the particles, a well-known phenomenon for TiO_2 [23]. It can be concluded from the spectrum (Figure 4a) that the photogenerated electrons mainly absorb

at higher wavelengths, as reported before [24]. This explains the observed differences in the spectra under Ar and methanol atmospheres.

$$CH_3OH \rightarrow {}^{\bullet}CH_2OH + H^+ + e^- . \quad (1)$$

For completeness, we note that in the absence of oxygen, the formed α-hydroxyl radicals react in a further step to produce formaldehyde (Equation (2)). This reaction possesses a redox potential of −1.41 V vs. NHE at pH 7 [22]. According to this potential, which is more negative than the flatband potential of K-7000 (−0.46 V vs. NHE), the formation of formaldehyde can occur by the injection of an electron into the conduction band of TiO_2, known as the current doubling effect [21].

$$^{\bullet}CH_2OH \rightarrow CH_2O + e^- + H^+ . \quad (2)$$

The transient absorption spectroscopy experiments using 455 nm light excitation offer a different picture. The photon energy (2.73 eV) is not sufficient for bandgap excitation in anatase TiO_2, as illustrated by the bandgap of K-7000 (3.31 eV). Accordingly, the pure anatase material UV100 shows no transient response after visible light excitation (Figure 6), with the exception of some experimental noise. On the contrary, a notable and long-lived signal can be detected in K-7000 under the same conditions, originated from its light absorption in the visible range, as described above. Regarding the physical origin of such absorption, we recall that investigations performed in the group of Prof. Kisch have determined that, in K-7000, carbon is not incorporated into the lattice, as originally thought, but is rather deposited on the surface in the form of a molecular sensitizer [15]. This important distinction may have a profound impact on the photocatalytic mechanism under visible light, since doping usually causes bandgap narrowing, as demonstrated, for instance, in N- and S-doped TiO_2 [25,26]. In agreement with the molecular sensitizer description, we found no bandgap narrowing for K-7000, but rather an absorption band in the visible range related to the sensitizer. Incidentally, the sensitizer–TiO_2 assembly can be treated akin to dye-sensitized solar cells, where the electronic structure of the former is characterized by defined HOMO (highest occupied molecular orbital) and LUMO (lowest unoccupied molecular orbital) levels [27]. Therefore, under excitation with visible light, the transition does not involve the valence band and the conduction band of TiO_2, but rather the HOMO and LUMO levels of the sensitizer.

In coincidence with the experiments using excitation with UV light, no difference in the spectra and decays in Ar and oxygen atmosphere was observed after visible light excitation of K-7000 (Figures 4 and 5). This indicates that no reaction takes place with oxygen in the considered time scale. A plausible explanation is that, after excitation of the carbon-based sensitizer, electrons are injected from the LUMO to the conduction band of TiO_2, as known for dye-sensitized solar cells [27]. Therefore, under visible light irradiation, oxygen reduction is ultimately limited in the same way as for bandgap excitation [19].

At odds with the transient absorption results using UV excitation, we observed no differences in the decays and spectra in methanol atmosphere with respect to inert atmosphere, indicating that no degradation of methanol takes place within the considered time scale under visible light excitation. Furthermore, the decays observed in all atmospheres after excitation with visible light were found to be rather long-lasting. This behavior is comparable to the decay obtained in methanol atmosphere after excitation with UV light (Figure 5a), where electrons accumulate in the TiO_2 particles. In the present case, electron transfer from the LUMO of the sensitizer to the conduction band of TiO_2 gives rise to their accumulation, since either no electron scavenger is present (Ar or methanol) or the rate of electron consumption is very low (O_2). Concomitantly, the radical cations of the sensitizer are produced after electron injection, which may lead to a bleaching of the sensitizer [28].

To obtain further insights into the oxidation of methanol over K-7000 under visible light irradiation (or the lack thereof), we performed photocatalytic experiments under continuous irradiation in aerated aqueous suspensions. After 60 min of irradiation in the presence of K-7000, less than 2% of a 100 μM methanol solution was transformed to formaldehyde (Figure 7 and Figure S2). These observations are

in good agreement with the transient absorption spectroscopy results, revealing that, under visible light irradiation, the degradation of methanol is negligible or, at best, slow. To understand this behavior, the possible degradation mechanisms of methanol under irradiation with UV light as well as visible light in the presence of the photocatalyst must be discussed. Generally, after excitation with UV light, electron–hole pairs are generated in the TiO_2 particles (Equation (3)). In this case, the carbon-based sensitizer is possibly excited as well. However, considering the smaller amount of the sensitizer layer compared to TiO_2, the excitation of the sensitizer can be neglected in the mechanism. The photogenerated electrons can react with oxygen molecules forming a superoxide radical ($O_2^{-\bullet}$) (Equation (4)), while the photogenerated holes can be trapped either at terminal protonated bridging oxygen ions (OH_{br}^-) to form a hydroxyl radical ($\text{-}OH_{br}^{\bullet}$) (Equation (5)) or at adsorbed methanol molecules (CH_3OH_{ads}) forming an α-hydroxyl radical ($^{\bullet}CH_2OH$) (Equation (6)). Methanol molecules in aqueous solution (CH_3OH_{aq}) can be oxidized via hydroxyl radicals yielding the same radical (Equation (7)). In an aerated suspension, the produced α-hydroxyl radicals are further oxidized to formaldehyde through reaction with oxygen molecules (Equation (8)) [29].

$$TiO_2 + h\nu \rightarrow e_{CB}^- + h_{VB}^+, \quad (3)$$

$$O_2 + e_{CB}^- \rightarrow O_2^{-\bullet}, \quad (4)$$

$$OH_{br}^- + h_{VB}^+ \rightarrow -OH_{br}^{\bullet}, \quad (5)$$

$$CH_3OH_{ads} + h_{VB}^+ \rightarrow {}^{\bullet}CH_2OH + H^+, \quad (6)$$

$$CH_3OH_{aq} + -OH_{br}^{\bullet} \rightarrow {}^{\bullet}CH_2OH + H^+, \quad (7)$$

$${}^{\bullet}CH_2OH + O_2 \rightarrow CH_2O + O_2^{-\bullet} + H^+. \quad (8)$$

On the other hand, after excitation with visible light the mechanism will be different, since the excitation energy is not enough to generate electron–hole pairs in TiO_2. Thus, under visible light irradiation, only the carbon-based sensitizer layer (CS) can be excited (CS^*), after which an electron is transferred from the LUMO to the conduction band of the TiO_2 (Equation (9)), simultaneously forming the radical cation of the sensitizer ($CS^{\bullet+}$). Afterwards, the electron in the conduction band can react with molecular oxygen (Equation (4)), while the sensitizer radical cation could react with methanol to form an α-hydroxyl radical ($^{\bullet}CH_2OH$) (Equation (10)). Exactly as after irradiation with UV light, this radical can react further with molecular oxygen, yielding formaldehyde (Equation (8)).

$$CS + h\nu \rightarrow CS^* \rightarrow CS^{\bullet+} + e_{CB}^-, \quad (9)$$

$$CS^{\bullet+} + CH_3OH \rightarrow CS + {}^{\bullet}CH_2OH. \quad (10)$$

However, the reaction shown in Equation (10) does not occur at a significant rate, since neither the transient absorption spectroscopy measurements nor the photocatalytic experiments suggest a degradation of methanol. The reason for the lack of reaction is discussed below. In passing, we represent the different reactions and processes occurring after excitation with UV and visible light in Scheme 1.

In contrast to methanol, chlorpromazine, which belongs to the phenothiazines group, could be completely degraded within the first 30 min of continuous visible light irradiation in the presence of K-7000 (Figure 7). In order to explain this difference, the mechanism of the visible light induced conversion of chlorpromazine must be taken into account. Upon visible light irradiation, excitation of the carbon-based sensitizer leads to electron transfer to the conduction band of TiO_2 (Equation (9)). In the presence of oxygen, these electrons (slowly) reduce it, forming superoxide radicals (Equation (4)). The sensitizer radical cation ($CS^{\bullet+}$) is able to oxidize chlorpromazine to form a chlorpromazine radical cation (Equation (11)), simultaneously regenerating the sensitizer. As reported for similar compounds [30], the next step is most likely the reaction between the produced chlorpromazine radical

cation and a superoxide radical to form a persulfoxide molecule (Equation (12)). The persulfoxide molecule forms a thiadioxirane (Equation (13)), which reacts with a further chlorpromazine molecule yielding two chlorpromazine sulfoxide molecules (Equation (14)), as expected from the mechanism proposed by Somasundaram and Srinivasan for the oxidation of aryl methyl sulfides in the presence of irradiated TiO_2 [30].

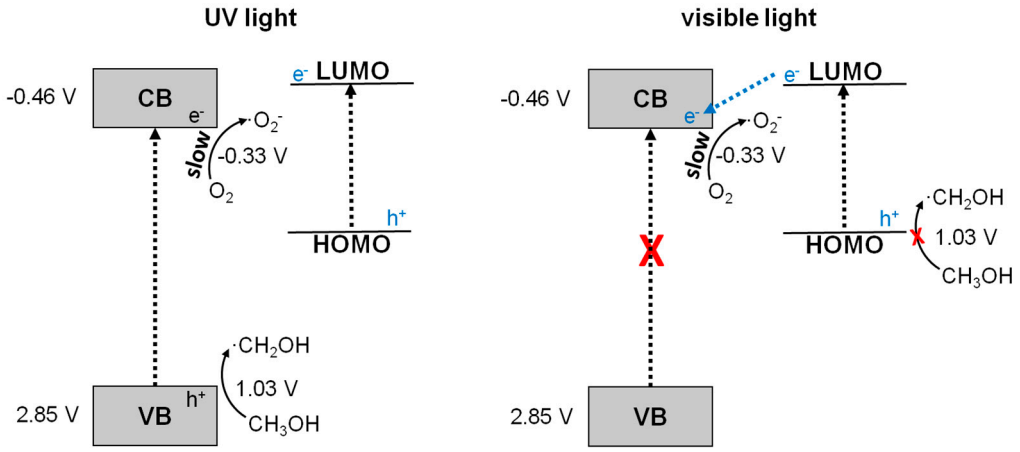

Scheme 1. Proposed processes taking place after excitation of K-7000 with UV light and visible light. The excitation with UV light leads to the generation of electron-hole pairs in the anatase particles and the carbon-based sensitizer as well, while visible light causes the excitation of the carbon-based sensitizer.

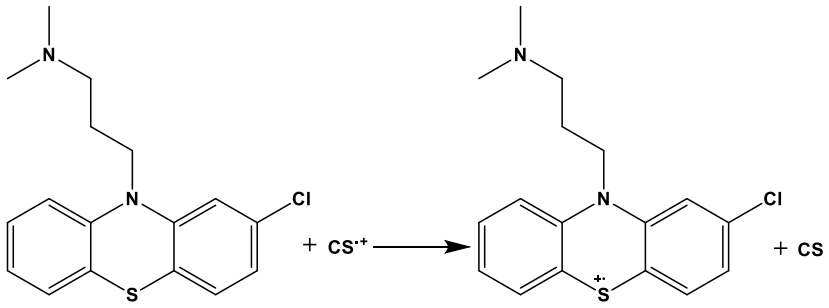

(11)

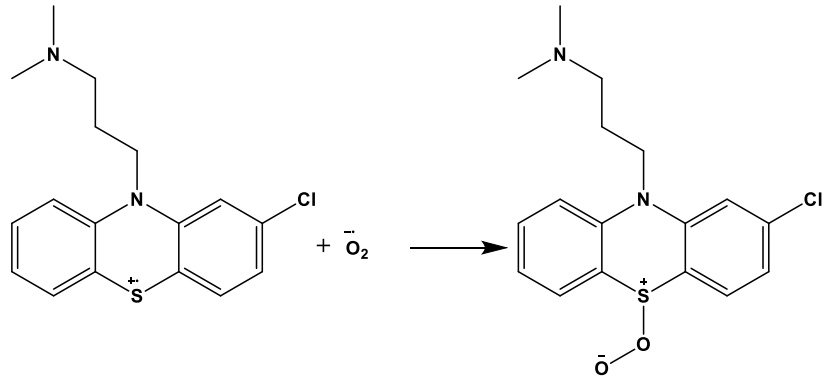

(12)

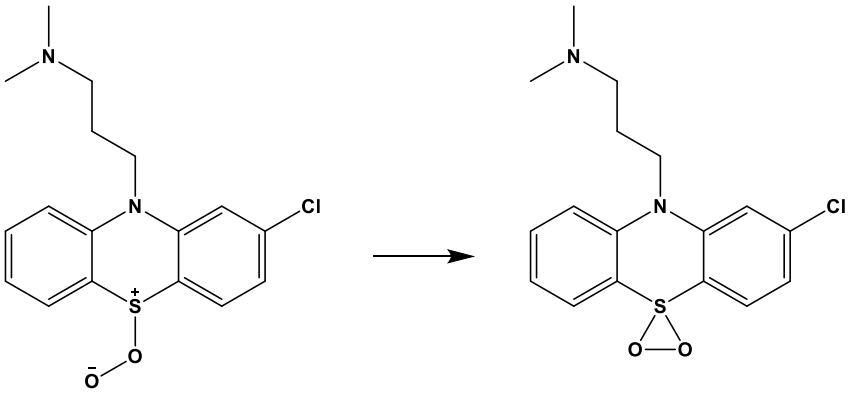

(13)

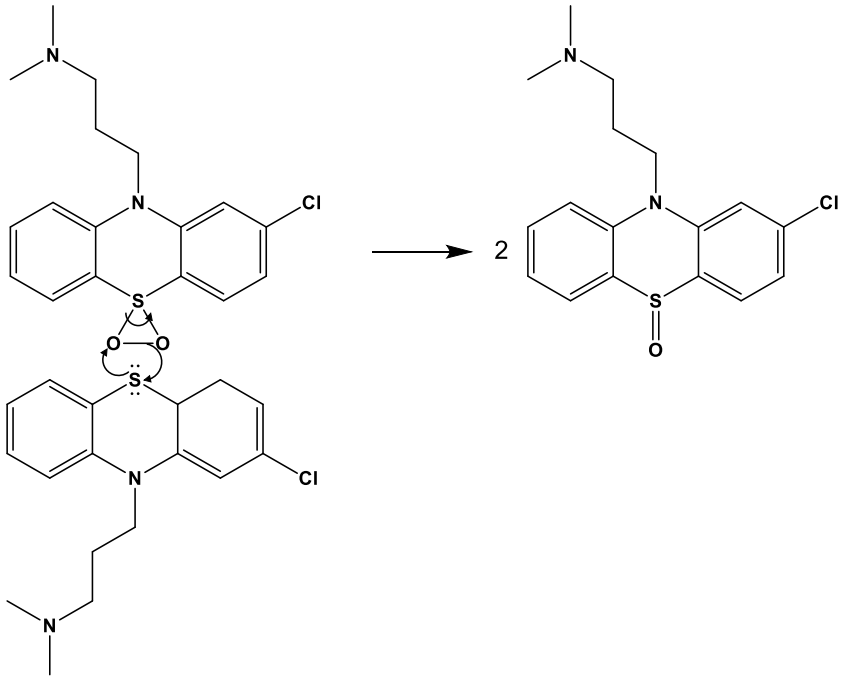

(14)

Contrary to methanol, which was not significantly oxidized upon visible light irradiation of K-7000, chlorpromazine is able to react with the sensitizer radical cation, yielding its sulfoxide. The reaction of the organic compound with the sensitizer radical cation is essential for the further photocatalytic reaction steps. If this initial reaction does not take place, the further steps will not occur as well. To explain the reason why this initial reaction only happens with chlorpromazine and not with methanol, the redox potentials for the corresponding reactions have to be considered. As mentioned before, the required potential for the methanol oxidation (Equation (1)) is 1.03 V vs. NHE at pH 7 [22]. The redox potential for the one-electron oxidation of chlorpromazine is 0.53 V vs. NHE at pH 7 and, thus, more negative [31,32]. From this information, it can be concluded that the redox potential of the sensitizer radical cation is more positive than that of the chlorpromazine oxidation and either more negative or close to that of the methanol oxidation, which hinders its reaction with the latter. We note that, being electron transfer reactions, their kinetics are governed by Marcus theory [33,34]. As such, even if the reaction is moderately exergonic, it still may occur at a reduced rate due to the influence of the solvent reorganization energy. Additionally, we can estimate that the position of the LUMO must be located at a more negative potential than the conduction band edge of TiO_2; otherwise, no electron transfer from the excited sensitizer to the conduction band of TiO_2 would be possible. However, it has to be mentioned that the exact position of the LUMO cannot be determined from these experiments. All relevant redox potentials, as well as the conduction band and valence band

position of the photocatalyst, including the possible positions of the LUMO and HOMO, are gathered in Scheme 2.

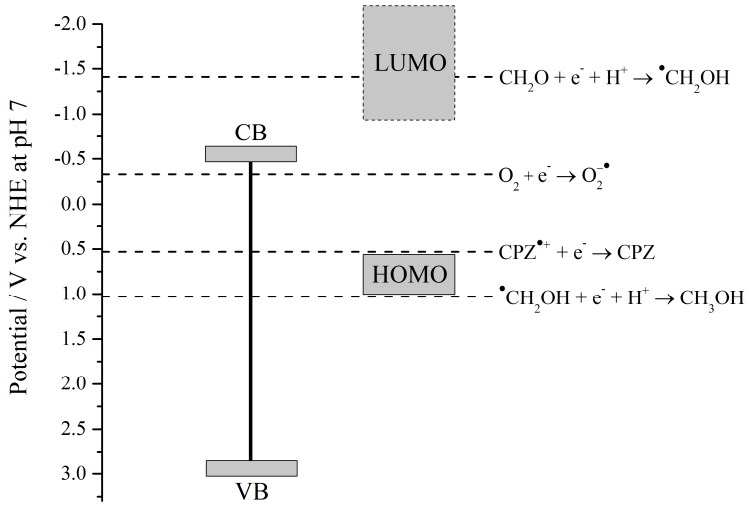

Scheme 2. Band positions of the anatase photocatalyst K-7000 with the corresponding redox potentials of the oxygen reduction, methanol oxidation, and chlorpromazine (CPZ) oxidation at pH 7 and the possible positions of the LUMO and the HOMO of the sensitizer [18,22].

To confirm the results of the photocatalytic experiments, we performed transient absorption spectroscopy measurements with the K-7000 powder in the presence of pre-adsorbed chlorpromazine. Unlike the case of methanol (Figure 5b), the transient absorption of bare K-7000 changes in the presence of chlorpromazine, giving rise to a signal attributable to the chlorpromazine radical cation [35] (Figure S7). Thus, both the continuous irradiation experiments and the transient absorption spectroscopy measurements evince a prompt degradation of chlorpromazine and a negligible one for methanol. We note that chlorpromazine oxidation under UV irradiation of K-7000 has been the subject of a recent study [36] and, thus, we focused here on its visible light degradation.

Interestingly, the oxidation product of the chlorpromazine degradation, namely chlorpromazine sulfoxide, was found to be highly persistent throughout the visible light irradiation of K-7000 (Figure S5). This product was found to be a long-lasting compound upon visible light driven photocatalysis as well, as previously reported [36]. This result can be understood on the same grounds as for methanol and chlorpromazine. Although the redox potential for the one-electron oxidation of chlorpromazine sulfoxide has not, to the best of our knowledge, been determined, potentials in the range of 2.5 V to 2.8 V have been reported for similar sulfoxides [30], i.e., very close to the valence band edge of K-7000. By assuming a potential for chlorpromazine sulfoxide in this range, no oxidation can be expected, since this value is located at a position even more positive than that for the methanol oxidation.

In summary, our results with the commercial photocatalyst K-7000 illustrate that photogenerated charge carriers in visible light active materials may have a limited ability to drive oxidation reactions, which is at odds with the general wisdom stating that photogenerated holes in TiO_2 possess a very high oxidizing power. Moreover, while this fact may be detrimental for the application of such materials in environmental remediation, it may however be exploited to increase the selectivity of the oxidation half-reaction in photocatalytic processes. Instead of complete mineralization, under the right conditions it might be possible to selectively oxidize an unwanted compound into a valuable one [37].

4. Materials and Methods

4.1. Chemicals

KRONOClean 7000, the carbon-modified TiO_2 powder, was provided by Kronos International, Inc. (Leverkusen, NRW, Germany). Hombikat UV100, a pure anatase TiO_2 photocatalyst, was provided by

Sachtleben Chemie GmbH (Duisburg, NRW, Germany). Chlorpromazine sulfoxide was purchased from LGC-Standards (Wesel, NRW, Germany) and acetonitrile (Rotisolv® HPLC Gradient) was purchased from Carl-Roth (Karlsruhe, BW, Germany). Chlorpromazine hydrochloride (CPZ) (≥98%), trifluoroacetic acid (Uvasol®, for spectroscopy), and all other chemicals in this work were purchased from Sigma-Aldrich (Merck, Darmstadt, HE, Germany) (unless noted) and were used as received. In all experiments ultrapure water (≥18.2 MΩ cm) was employed.

4.2. Characterization of K-7000

X-ray diffraction (XRD) analysis was performed using Cu K_α radiation (λ = 0.154178 nm) with a Bruker D8 Advance diffractometer. The patterns were recorded at room temperature in the 2θ range between 20° and 80°, with steps of 0.011° in Bragg–Brentano geometry (θ–θ). The diffuse reflectance spectra of the photocatalysts powders were determined in the spectral range from 300 to 800 nm by means of a Varian Cary-100 UV–vis spectrophotometer equipped with an integrating sphere, with barium sulfate as a reflectance reference. The optical bandgap was determined using a Tauc plot analysis assuming indirect transitions (Figure S1).

The flatband potential was determined through the Mott–Schottky method, performed using a ZENNIUM Electrochemical Workstation (ZAHNER-elektrik) with a 0.1 M KNO_3 solution as the electrolyte and a frequency of 100 Hz. For this measurement, a three-electrode electrochemical cell made of Teflon, with a Pt counter electrode and an Ag/AgCl/NaCl (3 M) reference electrode, was used. The screen-printing technique was applied to prepare the K-7000 and Hombikat UV100 films on a 3 cm × 3 cm fluorine-doped tin oxide (FTO) glass (Sigma-Aldrich) calcined at 450 °C, as the working electrode. The paste used to prepare the films was obtained following the procedure described by Ito et al. [38].

4.3. Transient Absorption Spectroscopy

The transient absorption spectroscopy measurements were performed with the catalyst powder inside a flat quartz cell. All samples were purged prior to the experiments with either argon, a mixture of nitrogen and methanol, or oxygen for 30 min. The experiments were performed in diffuse reflectance mode by means of an Applied Photophysics LKS 80 Laser Flash Photolysis Spectrometer with a pulsed Nd:YAG laser (Quantel, Brilliant B). For excitation of the samples, the third harmonic of the laser (355 nm, 6 ns pulses) or the third harmonic equipped with an optical parametric oscillator (OPO, 455 nm) was used with an average energy of 3 mJ·cm^{-2}. The laser light and the analyzing light (Xenon lamp, pulsed, Osram XBO, 150 W) were focused on the surface of the powder sample. The reflected light was guided to a detector (Hamamatsu PMT R928), which was connected with a 100 Ω resistance to an oscilloscope. The photomultiplier converted the incoming photons directly into a current. For every detection wavelength, a different voltage was applied to the photomultiplier to adjust the light level to a constant value. Absorbance values, Abs, were calculated from the reflected light before (J_0) and after the laser excitation (J). The values of the change of reflectance, ΔJ, were obtained by applying the following equation:

$$\Delta J = 1 - 10^{-Abs} = \frac{J_0 - J}{J_0} \quad (15)$$

For each detection wavelength, a time scale of 10 μs was considered, 25 shots were averaged and the data points were reduced to 200. The spectra were recorded from 400 nm to 650 nm in 25 nm steps for excitation with 355 nm and from 550 nm to 650 nm in 25 nm steps for the excitation with 455 nm.

4.4. Photocatalytic Procedure

For the photocatalytic experiments, chlorpromazine and methanol were chosen as probe organic molecules. The irradiation source was a monochromatic light emitting diode (LED) with an emission maximum at 455 nm (Thorlabs, M455L3, 339 W·m^{-2}; emission spectrum shown in Figure S5). The photocatalytic setup included a barrel-shaped borosilicate photoreactor (diameter: 6 cm, height:

3 cm) covered with a black polymer case, which had a connection on the top for the attachment of the LED light source. For these experiments, initially a 60 mL aqueous suspension of 100 μM chlorpromazine/methanol and 1 $g \cdot L^{-1}$ photocatalyst was prepared at its natural pH. The suspension was then stirred for 60 min under dark conditions in the photoreactor to reach the adsorption–desorption equilibrium. Afterwards, the LED light source began to irradiate the reaction medium for 60 min; throughout the reaction period, the suspension was purged with oxygen. At regular time intervals, samples were taken, centrifuged, and filtered (PVDF, 0.2 μm pore size). For the experiments with chlorpromazine, the samples were analyzed with a HPLC-UV-MS (ESI) device using an Alliance 2795-HT HPLC (Waters, UK) coupled with a 1050 UV-detector (type 79853C, detection wavelength: 254 nm, HP, USA) and an LCT Premier ESI mass spectrometer (Waters, UK). The resulting data of the conversion of chlorpromazine into its main product chlorpromazine sulfoxide were presented in terms of the change of their concentration (μM) versus irradiation time (min). For the methanol degradation, the production of formaldehyde was monitored by derivatizing it with Nash's reagent [39] and then following the colored product with a Varian Cary-100 UV–vis spectrophotometer. The conversion of methanol was compared with that of chlorpromazine in terms of the concentration at the sampling time divided by the initial concentration after the equilibrium ($C/C_{0,e}$). Photocatalytic experiments were performed at least twice to ensure reproducibility.

5. Conclusions

We studied the reactivity upon UV and visible light irradiation of the commercially available photocatalyst KRONOClean 7000. Its characterization revealed that its crystalline structure, flatband potential, and light absorption in the UV range closely match those of pure anatase TiO_2. Its visible light photocatalytic activity originates from a long-tailed absorption in this range, which is ascribed to the carbon modification employed for its preparation. By means of transient absorption spectroscopy, we investigated charge carrier generation and recombination in the material using Ar, O_2, and methanol atmospheres. Excitation with UV light did not show a significant reaction of photogenerated charge carriers with oxygen in the investigated time window, explained by a slow electron transfer. In the presence of methanol, we observed a gradual accumulation of electrons due to its fast reaction with photogenerated holes. Upon excitation with visible light, all spectra and decays show similar features, indicating that neither with methanol nor with O_2 a reaction takes place to a significant degree. Complementarily, we performed photocatalytic reactions under visible light irradiation, after which we observed no methanol oxidation, but a fast degradation of chlorpromazine. We rationalized these results by considering K-7000 akin to a dye-sensitized system, in which the carbon-based layer acts as a molecular sensitizer. As such, excitation with UV light leads to the generation of electron-hole pairs in TiO_2, while visible light causes the excitation of the sensitizer followed by electron injection into TiO_2 and subsequent formation of the radical cation. Ultimately, the oxidation ability of the material depends on the difference between the redox potential of the radical cation and that of the molecule to be oxidized: while the oxidation potential of methanol is too negative for it to react, that of chlorpromazine allows the reaction to swiftly occur.

All in all, our results show that excitation of the photocatalyst with visible light leads to a lower reactivity than for UV light, limited by the redox potential of the radical cation of the sensitizer. Moreover, although photogenerated charge carriers in this visible light active material may have a limited ability to drive oxidation reactions, under the right circumstances this could be exploited to increase the selectivity of photocatalytic transformations.

Supplementary Materials: The following are available online at http://www.mdpi.com/2073-4344/9/8/697/s1, Figure S1: Determination of the bandgap of K-7000 and UV100 via the Tauc plot, Figure S2: Kinetic profile for the formation of formaldehyde upon the photocatalytic oxidation of methanol (C_0 = 100 μM) under visible light irradiation in the presence of K-7000, Figure S3: Photolysis and photocatalytic conversion (in the presence of K-7000) of chlorpromazine under visible light irradiation, Figure S4: Absorption spectrum of a 100 μM aqueous solution of chlorpromazine (black line), and emission spectrum of the employed light source (blue line), Figure S5: Photocatalytic conversion of chlorpromazine to the main product chlorpromazine sulfoxide in the presence of

K-7000 under visible light irradiation, Figure S6: Photocatalytic conversion of chlorpromazine under visible light irradiation in the presence of K-7000 and Hombikat UV100, Figure S7: (**a**) Transient absorption decays of K-7000 observed at 550 nm and (**b**) transient absorption spectra of K-7000 measured at 100 ns after the laser excitation in an Ar atmosphere and in the presence of chlorpromazine after excitation with 455 nm.

Author Contributions: Conceptualization, A.A. and C.G.; methodology, A.A. and C.G.; validation, A.A. and C.G.; formal analysis, A.A. and C.G.; investigation, A.A., C.G., and M.C.; writing—original draft preparation, A.A. and C.G.; writing—review and editing, A.A., C.G., and M.C.; visualization, A.A. and C.G.; supervision, M.C. and D.B.

Funding: This research was supported by Saint-Petersburg State University via a research Grant ID 32706707. The publication of this article was funded by the Open Access fund of Leibniz Universität Hannover.

Acknowledgments: The authors are grateful to Dr. Gerald Dräger for performing the HPLC-MS measurements. A.A. acknowledges the financial support of the Deutscher Akademischer Austauschdienst (DAAD). C.G. acknowledges financial support from the Leibniz Universität Hannover within the program "Wege in die Forschung II". M.C. is grateful to the DAAD together with the Ministerio de Educación, Cultura, Ciencia y Tecnología (Argentina) for his ALEARG scholarship.

Conflicts of Interest: The authors declare no conflict of interest.

References

1. Fujishima, A.; Honda, K. Electrochemical photolysis of water at a semiconductor electrode. *Nature* **1972**, *238*, 37–38. [CrossRef] [PubMed]
2. Schneider, J.; Matsuoka, M.; Takeuchi, M.; Zhang, J.; Horiuchi, Y.; Anpo, M.; Bahnemann, D.W. Understanding TiO_2 Photocatalysis: Mechanisms and Materials. *Chem. Rev.* **2014**, *114*, 9919–9986. [CrossRef] [PubMed]
3. Pelaez, M.; Nolan, N.T.; Pillai, S.C.; Seery, M.K.; Falaras, P.; Kontos, A.G.; Dunlop, P.S.M.; Hamilton, J.W.J.; Byrne, J.A.; O'Shea, K.; et al. A review on the visible light active titanium dioxide photocatalysts for environmental applications. *Appl. Catal. B Environ.* **2012**, *125*, 331–349. [CrossRef]
4. Günnemann, C.; Haisch, C.; Fleisch, M.; Schneider, J.; Emeline, A.V.; Bahnemann, D.W. Insights into Different Photocatalytic Oxidation Activities of Anatase, Brookite, and Rutile Single-Crystal Facets. *ACS Catal.* **2019**, *9*, 1001–1012. [CrossRef]
5. Tayade, R.J.; Surolia, P.K.; Kulkarni, R.G.; Jasra, R.V. Photocatalytic degradation of dyes and organic contaminants in water using nanocrystalline anatase and rutile TiO_2. *Sci. Technol. Adv. Mater.* **2007**, *8*, 455–462. [CrossRef]
6. Grätzel, M.; Rotzinger, F.P. The Influence of the Crystal Lattice Structure on the Conduction Band Energy of Oxides of Titanium(IV). *Chem. Phys. Lett.* **1985**, *118*, 474–477. [CrossRef]
7. Reference Solar Spectral Irradiance: ASTM G-173. 2012.
8. Arimi, A.; Megatif, L.; Granone, L.I.L.I.; Dillert, R.; Bahnemann, D.W.D.W. Visible-light photocatalytic activity of zinc ferrites. *J. Photochem. Photobiol. A Chem.* **2018**, *366*, 118–126. [CrossRef]
9. Curti, M.; Kirsch, A.; Granone, L.I.; Tarasi, F.; López-Robledo, G.; Bahnemann, D.W.; Murshed, M.M.; Gesing, T.M.; Mendive, C.B. Visible-Light Photocatalysis with Mullite-Type Bi2(Al1– $xFe_x)_4O_9$: Striking the Balance between Bandgap Narrowing and Conduction Band Lowering. *ACS Catal.* **2018**, *8*, 8844–8855. [CrossRef]
10. Xu, A.; Gao, Y.; Liu, H. The Preparation, Characterization, and their Photocatalytic Activities of Rare-Earth-Doped TiO_2 Nanoparticles. *J. Catal.* **2002**, *207*, 151–157. [CrossRef]
11. Klosek, S.; Raftery, D. Visible Light Driven V-Doped TiO_2 Photocatalyst and Its Photooxidation of Ethanol. *J. Phys. Chem. B* **2001**, *105*, 2815–2819. [CrossRef]
12. O'Regan, B.; Grätzel, M. A low-cost, high-efficiency solar cell based on dye-sensitized colloidal TiO_2 films. *Nature* **1991**, *353*, 737–740. [CrossRef]
13. Cho, Y.; Choi, W.; Lee, C.; Hyeon, T.; Lee, H. Visible Light-Induced Degradation of Carbon Tetrachloride on Dye-Sensitized TiO_2. *Environ. Sci. Technol.* **2001**, *35*, 966–970. [CrossRef] [PubMed]
14. Chowdhury, P.; Moreira, J.; Gomaa, H.; Ray, A.K. Visible-Solar-Light-Driven Photocatalytic Degradation of Phenol with Dye-Sensitized TiO_2: Parametric and Kinetic Study. *Ind. Eng. Chem. Res.* **2012**, *51*, 4523–4532. [CrossRef]
15. Ząbek, P.; Eberl, J.; Kisch, H. On the origin of visible light activity in carbon-modified titania. *Photochem. Photobiol. Sci.* **2009**, *8*, 264–269.

16. Sankova, N.; Semeykina, V.; Selishchev, D.; Glazneva, T.; Parkhomchuk, E.; Larichev, Y.; Uvarov, N. Influence of Tetraalkylammonium Compounds on Photocatalytic and Physical Properties of TiO_2. *Catal. Lett.* **2018**, *148*, 2391–2407. [CrossRef]
17. Tobaldi, D.M.; Seabra, M.P.; Otero-Irurueta, G.; de Miguel, Y.R.; Ball, R.J.; Singh, M.K.; Pullar, R.C.; Labrincha, J.A. Quantitative XRD characterisation and gas-phase photocatalytic activity testing for visible-light (indoor applications) of KRONOClean 7000®. *RSC Adv.* **2015**, *5*, 102911–102918. [CrossRef]
18. Ilan, Y.A.; Czapski, G.; Meisel, D. The one-electron transfer redox potentials of free radical I. The oxygen/superoxide system. *Biochmica er Biophys. Acta* **1976**, *430*, 209–224. [CrossRef]
19. Yamakata, A.; Ishibashi, T.; Onishi, H. Water- and Oxygen-Induced Decay Kinetics of Photogenerated Electrons in TiO_2 and Pt/TiO_2: A Time-Resolved Infrared Absorption Study. *J. Phys. Chem. B* **2001**, *105*, 7258–7262. [CrossRef]
20. Schneider, J.; Bahnemann, D.W. Undesired Role of Sacrificial Reagents in Photocatalysis. *J. Phys. Chem. Lett.* **2013**, *4*, 3479–3483. [CrossRef]
21. Memming, R. Photoinduced Charge Transfer Processes at Semiconductor Electrodes and Particles. In *Electron Transfer I. Topics in Current Chemistry*; Mattay, J., Ed.; Springer: Berlin/Heidelberg, Germany, 1994; Volume 169, pp. 105–181.
22. Wang, C.; Pagel, R.; Bahnemann, D.W.; Dohrmann, J.K. Quantum Yield of Formaldehyde Formation in the Presence of Colloidal TiO_2-Based Photocatalysts: Effect of Intermittent Illumination, Platinization, and Deoxygenation. *J. Phys. Chem. B* **2004**, *108*, 14082–14092. [CrossRef]
23. Iorio, Y.D.; Aguirre, M.E.; Brusa, M.A.; Grela, M.A. Surface Chemistry Determines Electron Storage Capabilities in Alcoholic Sols of Titanium Dioxide Nanoparticles. A Combined FTIR and Room Temperature EPR Investigation. *J. Phys. Chem. C* **2012**, *116*, 9646–9652. [CrossRef]
24. Bahnemann, D.; Henglein, A.; Lilie, J.; Spanhel, L. Flash photolysis observation of the absorption spectra of trapped positive holes and electrons in colloidal titanium dioxide. *J. Phys. Chem.* **1984**, *88*, 709–711. [CrossRef]
25. Morikawa, T.; Asahi, R.; Ohwaki, T.; Aoki, K.; Taga, Y. Band-Gap Narrowing of Titanium Dioxide by Nitrogen Doping. *Jpn. J. Appl. Phys.* **2001**, *40*, L561–L563. [CrossRef]
26. Umebayashi, T.; Yamaki, T.; Itoh, H.; Asai, K. Band gap narrowing of titanium dioxide by sulfur doping. *Appl. Phys. Lett.* **2003**, *81*, 2–5. [CrossRef]
27. Qin, P.; Yang, X.; Chen, R.; Sun, L.; Marinado, T.; Edvinsson, T.; Boschloo, G.; Hagfeldt, A. Influence of π-Conjugation Units in Organic Dyes for Dye-Sensitized Solar Cells. *J. Phys. Chem. C* **2007**, *111*, 1853–1860. [CrossRef]
28. Youngblood, W.J.; Lee, S.-H.A.; Kobayashi, Y.; Hernandez-Pagan, E.A.; Hoertz, P.G.; Moore, T.A.; Moore, A.L.; Gust, D.; Mallouk, T.E. Photoassisted Overall Water Splitting in a Visible Light-Absorbing Dye-Sensitized Photoelectrochemical Cell. *J. Am. Chem. Soc.* **2009**, *131*, 926–927. [CrossRef]
29. Ahmed, A.Y.; Kandiel, T.A.; Ivanova, I.; Bahnemann, D. Photocatalytic and photoelectrochemical oxidation mechanisms of methanol on TiO_2 in aqueous solution. *Appl. Surf. Sci.* **2014**, *319*, 44–49. [CrossRef]
30. Somasundaram, N.; Srinivasan, C. Oxidation of aryl methyl sulfides and sulfoxides on irradiated TiO_2. *J. Photochem. Photobiol. A Chem.* **1998**, *115*, 169–173. [CrossRef]
31. Merkle, F.H.; Discher, C.A. Electrochemical Oxidation of Chlorpromazine Hydrochloride. *J. Pharm. Sci.* **1963**, *53*, 620–623. [CrossRef]
32. Bahnemann, D.; Asmus, K.-D.; Willson, R.L. Phenothiazine Radical-cations: Electron Transfer Equilibria with Iodide Ions and the Determination of One-electron Redox Potentials by Pulse Radiolysis. *J. Chem. Soc. Perkin Trans. II* **1983**, 1669–1673. [CrossRef]
33. Feldt, S.M.; Lohse, P.W.; Kessler, F.; Nazeeruddin, M.K.; Grätzel, M.; Boschloo, G.; Hagfeldt, A. Regeneration and recombination kinetics in cobalt polypyridine based dye-sensitized solar cells, explained using Marcus theory. *Phys. Chem. Chem. Phys.* **2013**, *15*, 7087–7097. [CrossRef] [PubMed]
34. Marcus, R.A. Chemical and Electrochemical Electron-Transfer Theory. *Annu. Rev. Phys. Chem.* **1964**, *15*, 155–196. [CrossRef]
35. Maruthamuthu, P.; Sharma, D.K.; Serpone, N. Subnanosecond relaxation dynamics of 2,2′-azinobis (3-ethylbenzothiazoline-6-sulfonate) and chlorpromazine. Assessment of photosensitization of a wide band gap metal oxide semiconductor TiO_2. *J. Phys. Chem.* **1995**, *99*, 3636–3642. [CrossRef]

36. Arimi, A.; Dillert, R.; Dräger, G.; Bahnemann, D.W. Light-Induced Reactions of Chlorpromazine in the Presence of a Heterogeneous Photocatalyst: Formation of a Long-Lasting Sulfoxide. *Catalysts* **2019**, *9*, 627. [CrossRef]
37. Lang, X.; Chen, X.; Zhao, J. Heterogeneous visible light photocatalysis for selective organic transformations. *Chem. Soc. Rev.* **2014**, *43*, 473–486. [CrossRef] [PubMed]
38. Ito, S.; Chen, P.; Comte, P.; Nazeeruddin, M.K.; Liska, P.; Péchy, P.; Grätzel, M. Fabrication of screen-printing pastes from TiO_2 powders for dye-sensitised solar cells. *Prog. Photovoltaics Res. Appl.* **2007**, *15*, 603–612. [CrossRef]
39. Nash, T. The colorimetric estimation of formaldehyde by means of the Hantzsch reaction. *Biochem. J.* **1953**, *55*, 416–421. [CrossRef]